Pharmaceutical Research, Vol. 22, No. 2, February 2005 (© 2005)
DOI: 10.1007/s01869-005-1869-8

Research Paper

Estimation of the Three-Dimensional Pharmacophore of Ligands for Rat Multidrug-Resistance–Associated Protein 2 Using Ligand-Based Drug Design Techniques

Shuichi Hirono,[1,3] Izumi Nakagome,[1] Rie Imai,[1] Kazuya Maeda,[2] Hiroyuki Kusuhara,[2] and Yuichi Sugiyama[2]

Received March 22, 2004; accepted July 19, 2004

Purpose. Multidrug-resistance–associated protein 2 (Mrp2) shows a broad substrate specificity toward amphiphilic organic anions. This study identified key functional groups of ligand molecules for binding to rat Mrp2, determined their relative locations, and examined substrate specificity through receptor mapping using three-dimensional (3D) quantitative structure-activity relationship (3D-QSAR) analysis.
Methods. Ligand-binding conformations were estimated using conformational analysis (CAMDAS) and molecular superposition (SUPERPOSE) methods to clarify the substrate specificity of rat Mrp2 in relation to 3D ligand structures.
Results. Two types of binding conformations of ligands for rat Mrp2 were identified. 3D-QSAR comparative molecular-field analysis (CoMFA) revealed a statistically significant model for one type, in which the steric, electrostatic, and log P contributions to the binding affinity for rat Mrp2 were 63.0%, 33.4%, and 3.6%, respectively ($n = 16$, $q^2 = 0.59$, $n = 3$, $r^2 = 0.99$, and $s = 0.08$).
Conclusions. The 3D pharmacophore of ligands for rat Mrp2, and the ligand-binding region of rat Mrp2, were estimated. Ligand recognition of rat Mrp2 is achieved through interactions in two hydrophobic and two electrostatically positive sites (primary binding sites). The broad substrate specificity of rat Mrp2 might result from the combination of secondary (two electrostatically positive and two electrostatically negative sites) and primary binding sites.

KEY WORDS: binding conformation; 3D pharmacophore; 3D-QSAR; rat Mrp2; substrate specificity.

INTRODUCTION

The liver is one of the most important organs in the detoxification of xenobiotics, and biliary excretion is a major pathway for their elimination. Compounds in the circulating blood are taken up by hepatocytes and are then metabolized and/or excreted into the bile. Many kinds of drugs and their metabolites are transported across the sinusoidal and bile canalicular membranes via carriers. The mechanism of transport across the bile canalicular membrane has been characterized using isolated canalicular membrane vesicles (CMVs), which revealed that several types of primary active transporters are responsible for ligand efflux from the hepatocytes into the bile. Among them, multidrug-resistance–associated protein-2 (Mrp2; gene symbol ABCC2) has an important role in the biliary excretion of many organic anions and glutathione or glucuronide conjugates (1–3).

Mrp2 is an ATP-binding cassette (ABC) transporter, which possesses two highly conserved ABC regions. The Eisai hyperbilirubinemic rat (EHBR), which has a hereditary Mrp2 deficiency owing to the insertion of a nonsense mutation (4), and the GY/TR$^-$ rat (5) have both helped to reveal the importance of Mrp2 in the biliary excretion of various types of organic anions. In the EHBR, the biliary excretion of Mrp2 substrates is drastically decreased, and the ATP-dependent uptake of Mrp2 substrates into CMVs prepared from EHBRs is greatly reduced compared with those prepared from normal rats.

These findings demonstrate that a wide range of organic anions can be substrates for Mrp2, which include: nonconjugated organic anions such as dibromosulfophthalein (6,7), cefodizime (β-lactam antibiotic) (7), pravastatin (a 3-hydroxy-3-methyl-glutaryl-coenzyme A reductase inhibitor) (8), temocaprilat (an angiotensin-converting enzyme inhibitor) (9), the carboxylate forms of CPT-11 and its active metabolite (SN-38, which is a topoisomerase inhibitor) (8), and a cyclic anionic peptide (BQ-123, which is an endothelin antagonist) (10); glutathione conjugates such as leukotriene C_4 (11) and DNP-SG (12); and glucuronide conjugates such as bilirubin glucuronide (13), E3040 glucuronide (14,15), and SN-38 glucuronide (16).

[1] School of Pharmaceutical Sciences, Kitasato University, Tokyo 108-8641, Japan.
[2] Graduate School of Pharmaceutical Sciences, University of Tokyo, Tokyo 113-0033, Japan.
[3] To whom correspondence should be addressed. (e-mail: hironos@pharm.kitasato-u.ac.jp)

ABBREVIATIONS: ABC, ATP-binding cassette; CAMDAS, Conformational Analyzer with Molecular Dynamics and Sampling; C log P, calculated log P; CMVs, canalicular membrane vesicles; CoMFA, comparative molecular-field analysis; EHBR, Eisai hyperbilirubinemic rat; MD, molecular dynamics; Mrp2, multidrug-resistance–associated protein 2; PLS, partial least squares; QSAR, quantitative structure-activity relationship; rmsd, root-mean-square deviation; SD, Sprague-Dawley.

Clearly, rat Mrp2 accepts many organic anions as substrates. However, its broad substrate specificity has not been investigated in terms of the three-dimensional (3D) structures of ligands (17), and the complete 3D structure has not been determined for any mammalian transporter. Elucidating the structural characteristics of the ligand-binding region of rat Mrp2 would be useful for understanding its broad substrate specificity. Therefore, in the current study, we investigated the binding conformation of ligands to rat Mrp2, the key functional groups for binding to Mrp2 (3D pharmacophore), and the 3D quantitative structure-activity relationships (3D-QSAR) between ligands and rat Mrp2. Our combined method comprised the following three procedures: first, conformational analysis (CAMDAS) (18); second, a molecular superposition procedure (SUPERPOSE) (19); and third, 3D-QSAR analysis by comparative molecular-field analysis (CoMFA) (20). These techniques are described in more detail in the following section.

MATERIALS AND METHODS

Conformational Analysis: Sampling of a Set of Conformers of a Molecule

X-ray structural analysis of protein-ligand complexes has revealed that the binding conformation is one of the stable conformations of a ligand molecule. To generate a set of conformers of ligands, we used the automated program Conformational Analyzer with Molecular Dynamics and Sampling (CAMDAS), which was developed by Tsujishita and Hirono (18). CAMDAS performs high-temperature molecular dynamics (MD) calculations for a target molecule and for sampled conformers that appear during the MD. It then evaluates the similarities between each of the sampled conformers in terms of dihedral angle values, clusters similar conformers together, and, finally, prints out the clustered conformers. In this way, CAMDAS can find the representative conformers from an arbitrarily given structure of the molecule.

To estimate the binding conformation of ligands to rat Mrp2, MD dynamics calculations were executed for 18 ligands (a training set for constructing QSAR models comprising compounds **1**–**16** and a test set for verifying the QSAR models comprising compounds **A** and **B**), and many conformers were sampled; their chemical structures are shown in Figs. 1 and 2. An MD calculation for sampling was performed for 800 ps with an integral time step of 0.001 ps using an MM2 force field (21) without electrostatic and hydrogen-bonding interactions. The temperature of the system was maintained at 1200 K, and the length of the covalent bonds was fixed using the SHAKE algorithm throughout the MD simulations. Conformers were sampled at every 100 steps and preclustered with dihedral angles during the MD simulations. If the difference between conformers was within ±30°, they were grouped together. Subsequently, reclustering of the sampled conform-

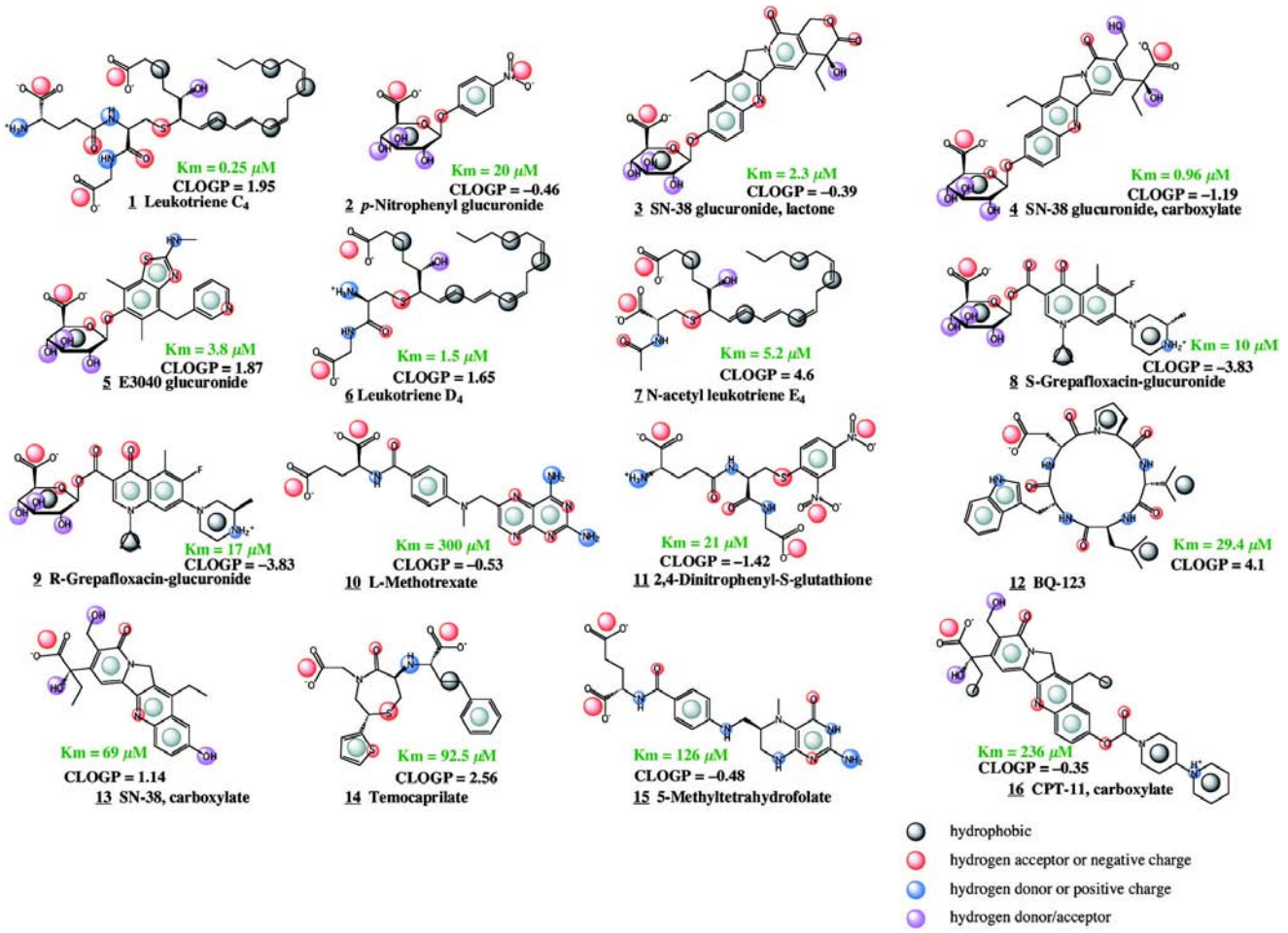

Fig. 1. Chemical structures of the compounds in the training set, with property spheres, K_m, and C log P values.

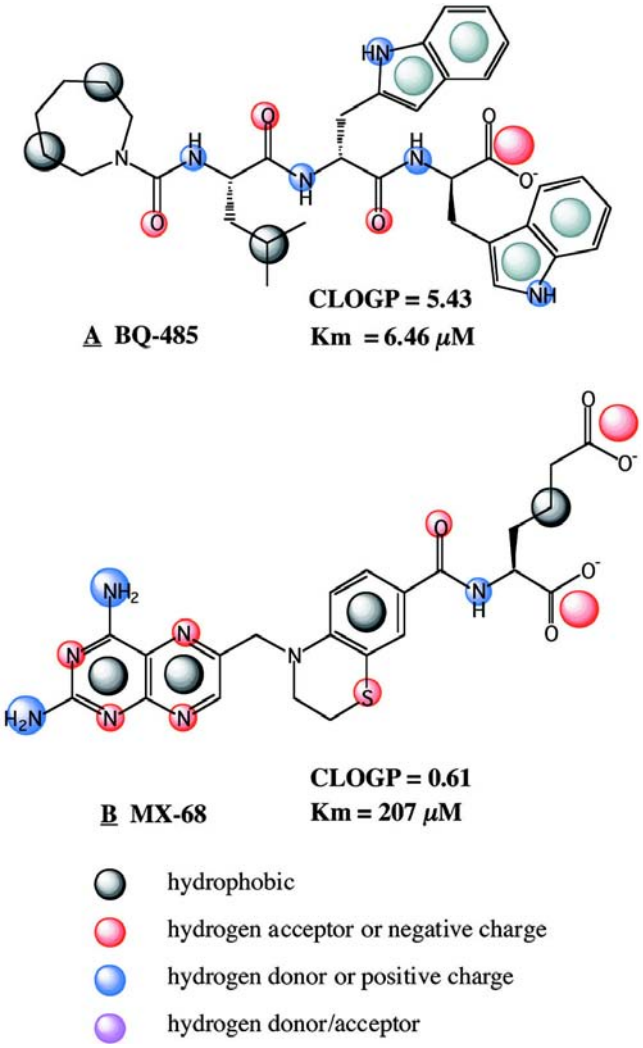

Fig. 2. Chemical structures of the compounds in the test set, with property spheres, K_m, and C log P values.

ers was performed with dihedral angles within ±30°. Before the clustering, each conformer was minimized until the root-mean-square (rms) of the gradients of the potential energy was below 0.004 kcal mol^{-1} $Å^{-1}$.

Molecular Superposition: Selection of the Candidate Binding Conformations

X-ray crystallographic studies of protein-ligand complexes have demonstrated that when ligands bind to a given protein, such as a receptor or a transporter, the atomic groups in the ligands that interact with amino-acid residues of the protein occupy the same 3D space. Based on this information, we carried out molecular superposition for ligand molecules using the SUPERPOSE program developed by Iwase and Hirono (19). The program superposes two molecules based on the physicochemical properties of the atomic groups, which is useful for elucidating a pharmacophore and estimating a binding conformation by distinguishing it from among the many conformations that are generated by high-temperature MD calculations.

Five types of physicochemical properties are considered in the program, including hydrophobic (aromatic), hydrogen-bond donors, hydrogen-bond acceptors, and hydrogen-bond donors/acceptor. Each type is represented as a sphere with a predefined radius and is assigned to a functional group in a molecule. After molecular superposition, the overlaps of the spheres are scored.

The program works as follows. First, a large molecule with its physicochemical properties represented by spheres is fixed at the center of a large box, and another smaller molecule, also with spheres representing its physicochemical properties, is translated and rotated in the box. The translational increment is 1 Å, and the center of mass is translated onto the body-centered-cubic lattice-points made in the circumscribed large-volume rectangular box. The rotation is performed on each of the lattice points. The ranges of the three Eulerian angles are $0° \leq \phi, \varphi < 360°$, and $0° \leq \theta \leq 180°$. The rotational increment is 4°. Second, at every translation or rotation, the property spheres that overlap are determined by calculating the distances between the spheres of the molecules. Third, overlaps of the spheres are scored so that points are added when atomic groups with the same physicochemical properties overlap, and points are subtracted when atomic groups with different physicochemical properties overlap, according to the scoring table (19). Atomic groups without overlaps are not scored.

These three operations are repeated to determine the orientation with the highest score and the smallest rms deviation (rmsd) of the distances of the overlapped atomic groups between the two molecules.

3D-QSAR Analyses: Determination of the Binding Conformation Using CoMFA

The SUPERPOSE program identified several plausible binding conformations. We therefore carried out comparative molecular field analysis (CoMFA) to determine the binding conformation of ligands to rat Mrp2 and to obtain 3D structure-activity relationships.

Table I. Results of Conformational Analysis by CAMDAS

	Number of conformers	ΔE (kcal/mol)	Number of conformers within 12 kcal/mol
Training set			
1	7777	15.570	3846
2	16	14.406	15
3	262	18.565	234
4	876	18.877	798
5	251	16.972	240
6	7777	13.951	5723
7	3121	1112.579	1576
8	479	54.432	316
9	264	32.593	180
10	2547	1013.488	2387
11	3957	978.039	3530
12	5937	53.872	1533
13	177	13.669	176
14	3078	52.334	2832
15	3069	1028.764	2915
16	5135	32.084	3856
Test set			
A	36	480.492	20
B	7777	86.823	4966

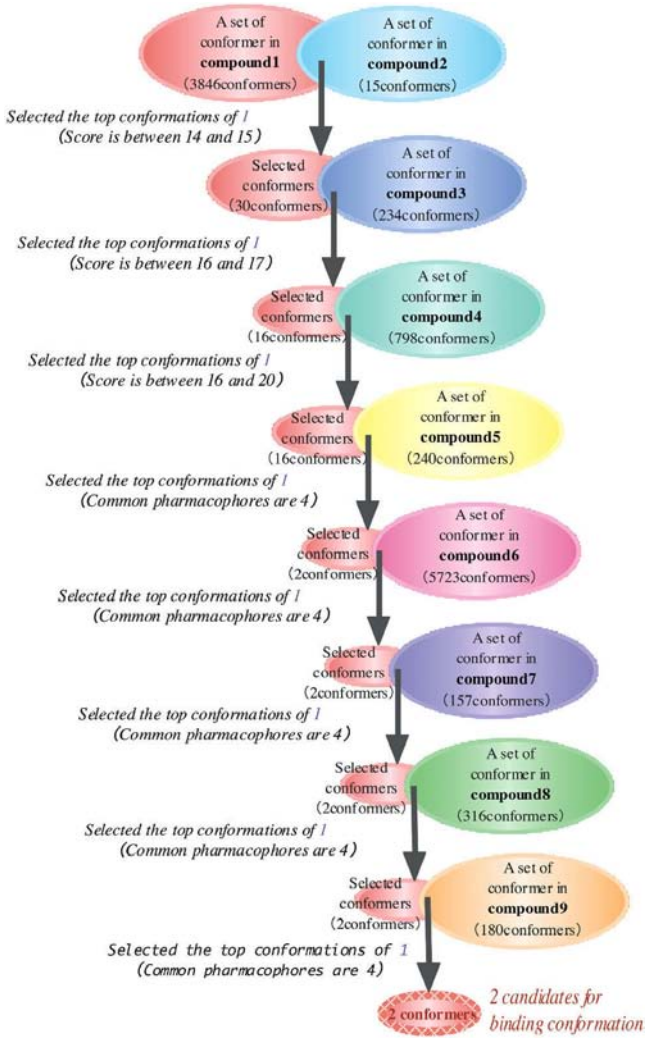

Fig. 3. Flowchart of SUPERPOSE.

The atomic charges of each conformer were calculated using the semiempirical molecular orbital program package MOPAC93 MNDO/ESP, in order to evaluate the electrostatic field in CoMFA. Conventional CoMFA was performed using the QSAR option of SYBYL (Tripos, Inc., St. Louis, MO, USA), with the Michaelis constant (K_m) (22) of each ligand included as bioactive data, as shown in Figs. 1 (training set) and 2 (test set). For the K_m-determination experiments, CMVs were prepared from male Sprague-Dawley (SD) rats, and the transport study was performed using the rapid-filtration technique, as described previously (11,12). All of the compounds were mainly excreted into the bile via rat Mrp2, as biliary excretion in EHBRs and/or the ATP-dependent uptake of each compound into CMVs prepared from EHBRs was disrupted. Therefore, the K_m values for the uptake into CMVs prepared from SD rats corresponded to those for rat Mrp2.

Two calculations were carried out, using an sp^3 carbon probe atom with a charge of +1 and either the steric and electrostatic components or the steric, electrostatic, and calculated log P (C log P) components. The calculated values of log P were estimated using the CLOGP program (Daylight, C.I.S. Inc., Rochester, NY, USA). The CoMFA QSAR equations were calculated with the partial least squares (PLS) algorithm. The optimal number of components in the final CoMFA PLS model was determined using the cross-validated R^2 (q^2) values obtained from the leave-one-out cross-validation technique. The CoMFA PLS model with the highest q^2 values was selected to estimate the binding conformation of ligands for rat Mrp2.

RESULTS

Sampling of a Set of Conformers of Each Ligand

Using the CAMDAS program, we carried out conformational analyses of ligand molecules bound to rat Mrp2. The high-temperature MD calculation was used with a potential function without an electrostatic interaction term and a hydrogen-bonding term to avoid undesirable intramolecular interactions (Figs. 1 and 2). The CAMDAS calculations gave many conformers of the 18 compounds, as shown in Table I. The sets of conformers of compounds **1**–**9**, the structures of which were significantly different from one another and showed relatively low K_m values, were used by the SUPERPOSE

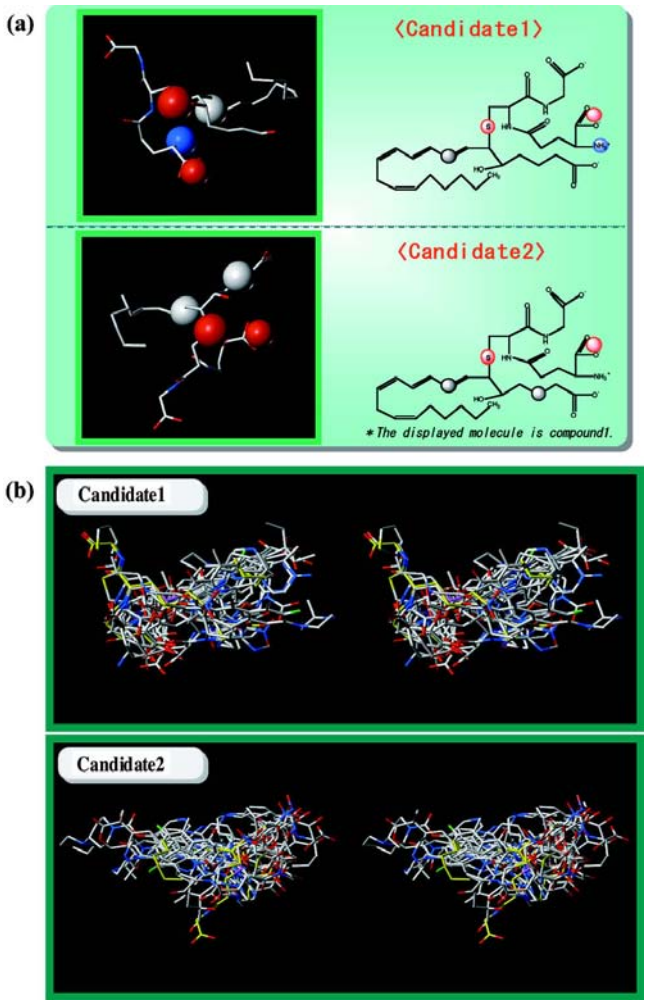

Fig. 4. (a) Property spheres common to compounds **1**–**9**. (b) Stereo views of superposed compounds in the training set (yellow molecule: compound **1**).

Table II. Results of CoMFA

Field type		Candidate 1		Candidate 2	
		ST + EL	ST + EL + C log P	ST + EL	ST + EL + C log P
Cross-validated	q^2	0.03	0.01	0.36	0.59
	s_{press}	1.21	1.15	0.80	0.64
No. of components		7	6	3	3
Conventional	r^2	1.00	1.00	0.99	0.99
	F	30122.14	2114.33	485.66	613.30
	s	0.01	0.03	0.09	0.08
Contribution (%)	ST	56.6	53.1	60.2	63.0
	EL	43.4	40.5	39.8	33.4
	C log P[a]	—	6.4	—	3.6

St, steric field; EL, electrostatic field; CoMFA, comparative molecular-field analysis.
[a] log P calculated by CLOGP.

program to determine the 3D pharmacophore of the ligand and to obtain the candidate binding conformations.

Selection of Candidate Binding Conformations

As shown in Table I, relatively stable conformers with molecular energies within 12 kcal/mol from the global minimum were selected as the conformers to be superposed. The cutoff value of 12 kcal/mol was confirmed in our previous study (19). For each ligand, the atomic groups that the property spheres were assigned to are shown in Figs. 1 (training set) and 2 (test set).

Initially, 3846 conformers of compound **1** and 15 conformers of compound **2** were superposed (Fig. 3). Each overlap was ranked on the basis of the SUPERPOSE score and the rmsd. As a result, we selected 30 conformers of compound **1** that represented good overlaps, with scores ranging between 14 and 15. Next, these 30 conformers of compound **1** and 234 conformers of compound **3** were superposed. As a result, we selected 16 conformers of compound **1** that showed good overlaps with conformers of compound **3**, with scores ranging between 16 and 17. The 16 selected conformers of compound **1** were then superposed to 798 conformers of compound **4**. No change was observed in the number of good overlaps at this stage, with scores ranging between 16 and 20 for all of the conformers. All 16 conformers of compound **1** were therefore superposed with 240 conformers of compound **5**. There were only two good overlaps for the superposition of compound **1** with compound **5**, with four commonly overlapped functional groups. Using the same method, the selected conformers of compound **1** were superposed to conformers of compounds **6**–**9** (Fig. 3). We finally obtained two conformers of compound **1** that were considered to be good candidates for the binding conformation. Figure 4a shows the common property spheres; namely, the pharmacophores obtained by superposition using compounds **1**–**9**.

Next, each candidate for the binding conformation was superposed to conformers of compounds **10**–**16** in the training set. The atomic groups that the ligand property spheres were assigned to are shown in Fig. 1. In this way, candidate binding conformations of compounds **10**–**16** were obtained. We then estimated the molecular alignment of ligand molecules (compounds **1**–**16**) that were essential to CoMFA (Fig. 4b). The

Table III. The Values of $\log(1/K_m)$ Calculated Using the Final CoMFA QSAR Model Compared with Experimental Data

	Experimental	Calculated	Residual
Compounds in the training set			
1 Leukotriene C4	6.60	6.70	–0.10
2 *p*-Nitrophenyl glucuronide	4.70	4.60	0.10
3 SN-38 glucuronide, lactone	5.64	5.63	0.01
4 SN-38 glucuronide, carboxylate	6.02	5.90	0.12
5 E3040 glucuronide	5.42	5.36	0.06
6 Leukotriene D4	5.82	5.77	0.05
7 *N*-acetyl leukotriene E4	5.28	5.33	–0.05
8 (*S*)-Grepafloxacin-glucuronide	5.00	5.00	0.00
9 (*R*)-Grepafloxacin-glucuronide	4.77	4.83	–0.06
10 L-Methotrexate	3.52	3.47	0.05
11 2,4-Dinitrophenyl-*S*-glutathione	4.68	4.76	–0.08
12 BQ-123	4.53	4.46	0.07
13 SN-38, carboxylate	4.16	4.25	–0.09
14 Temocaprilate	4.03	4.09	–0.06
15 5-Methyltetrahydrofolate	3.90	3.84	0.06
16 CPT-11, carboxylate	3.63	3.69	–0.06
Compounds in the test set			
A BQ-485	5.19	5.10	0.09
B MX-68	3.68	4.16	–0.48

two candidates of binding conformation of ligands for rat Mrp2 generated two types of molecular alignments, as shown in Fig. 4b. We also obtained binding conformation candidates for compounds **A**–**B** for the test set using a similar method to the training set. The test set was used to evaluate the predictive power of the CoMFA model obtained using the training set.

Determination of the Binding Conformation by CoMFA

CoMFA calculations were carried out using the two molecular alignments. The atomic charges of each conformer were calculated using MOPAC93 MNDO/ESP to evaluate the electrostatic field in CoMFA. Conventional CoMFA was performed with the QSAR option of SYBYL. For each molecular alignment (candidate 1 and candidate 2), two types of calculations were carried out together with an sp^3 carbon probe atom with a +1 charge: the first used steric and electrostatic fields, and the second used steric and electrostatic fields along with calculated values of log P (C log P). The CoMFA QSAR equations were calculated with the PLS algorithm. The optimal number of components in the final CoMFA PLS model was determined using the cross-validated R^2 (q^2) values obtained by the leave-one-out technique. The cross-validated R^2 (q^2) values, the standard error of the predictive sum of squares (s_{press}), and the standard error of the estimate (r^2) are listed in Table II for each candidate. The CoMFA PLS model with the highest q^2 values was assumed to best explain the binding conformation.

A good CoMFA model with three PLS components was obtained using the steric and electrostatic fields along with C log P for candidate 2. The final CoMFA model had a q^2 value of 0.59 with six PLS components, an s_{press} value of 0.64, an r^2 value of 0.99, and a standard error of 0.08. The experimental and calculated values of $\log(1/K_m)$ for each compound in the training set are listed in Table III. The property spheres shown in Fig. 5 illustrate the important atomic groups for the binding of each ligand molecule to rat Mrp2.

We also investigated the predictivity of the final CoMFA model using the test set of compounds. The values of $\log(1/K_m)$ calculated using the CoMFA model of candidate 2 with the steric field, electrostatic field, and C log P showed good agreement with the experimental values (Table III). We therefore concluded that the 3D structure of candidate 2 reflects the binding conformation of ligands for rat Mrp2. In the test set, the calculated value of $\log(1/K_m)$ for BQ-485 (5.10) compared well with the experimental value (5.19), whereas the calculated value of MX-68 contained a larger error (0.48). This might be the result of the difficulties of determining the atomic charges of MX-68, which has a pteridine ring, using MOPAC93 MNDO/ESP.

Figure 6a shows a contour map of the steric field from the final CoMFA model, together with the binding conformation of compound **1**: the green contours indicate areas in which bulky atomic groups are sterically favorable for the binding affinity, and the yellow contours indicate areas in which bulky groups are unfavorable for the binding affinity. Figure 6b shows a contour

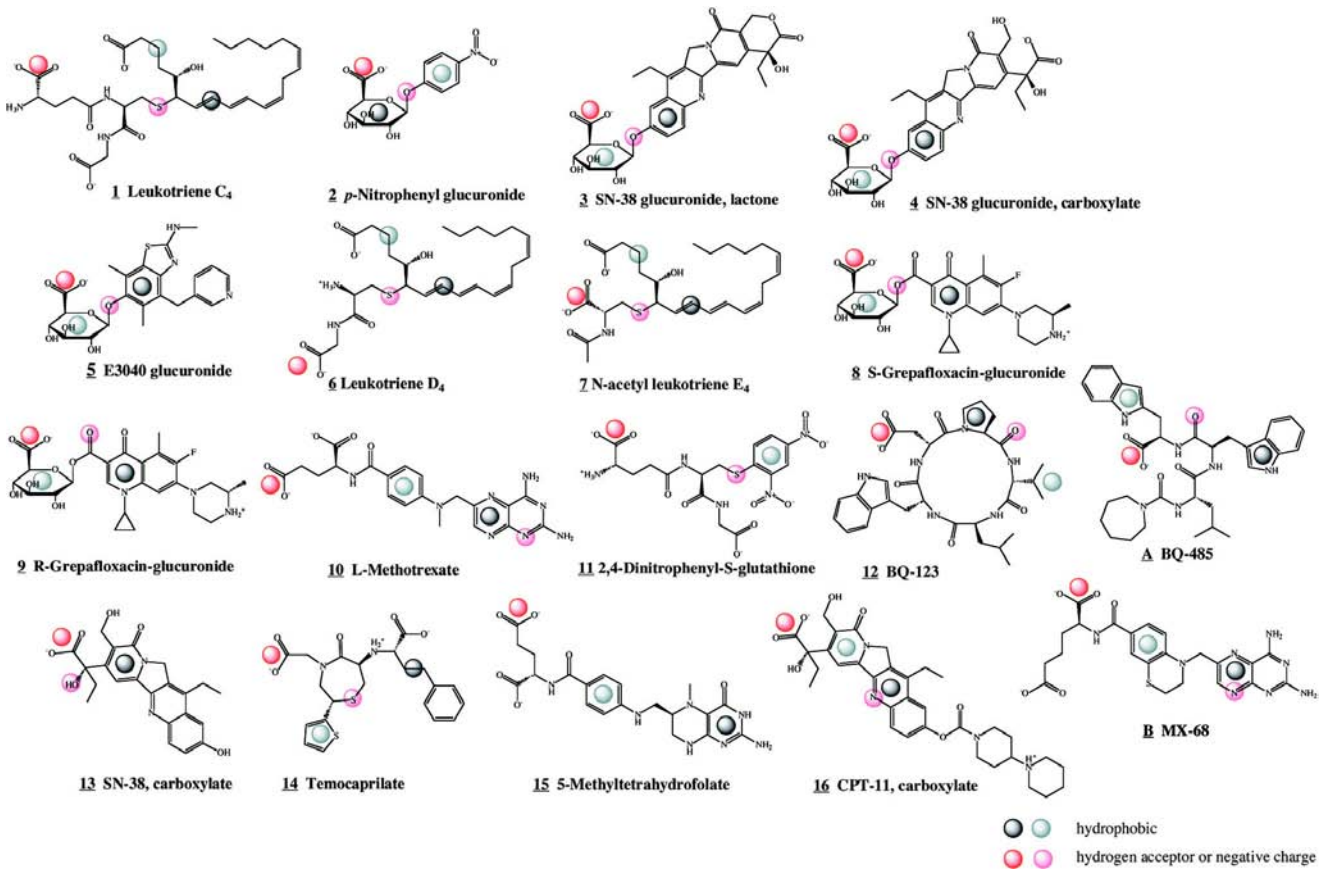

Fig. 5. Atomic groups involved in the binding of each ligand molecule to Mrp2/ABCC2.

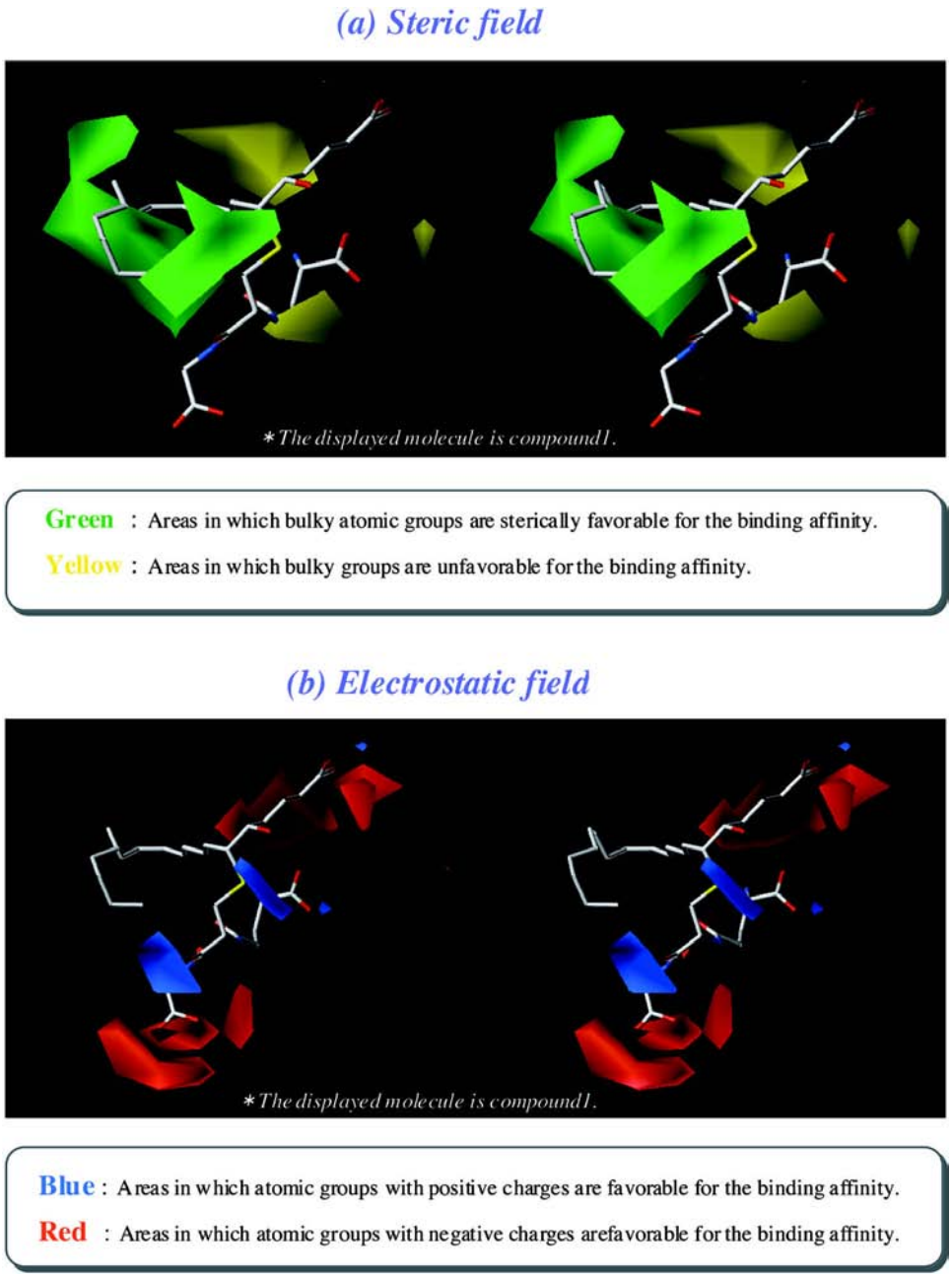

Fig. 6. Stereo views of contour maps obtained from the final CoMFA model. (a) Steric field. (b) Electrostatic field.

map of the electrostatic field from the final CoMFA model, together with the binding conformation of compound **1**: the blue contours indicate areas in which atomic groups with positive charges are advantageous to the binding of ligand with rat Mrp2, and the red contours show areas in which atomic groups with negative charges are favorable for the binding of ligand with rat Mrp2. The areas shown in the contour map are of great importance for explaining variation in the binding affinities of ligands with rat Mrp2.

DISCUSSION

Pharmacophore of Ligands for Rat Mrp2

We have identified a plausible binding conformation of ligands to rat Mrp2 by making full use of ligand-based drug design techniques. In this conformation, four property spheres that are common to all ligands were identified using the SUPERPOSE calculation. We propose that the spatial arrangement of the four functional groups expressed by these property spheres represents a 3D pharmacophore of ligands for rat Mrp2. Figure 7 shows a stereo view of these four property spheres along with the 3D structure of compound **1** and its structural formula. It appears that two hydrogen bond–acceptor groups (HA1 and HA2) and two hydrophobic groups (HP1 and HP2) are essential for the binding of ligands to rat Mrp2 and that these groups constitute the 3D pharmacophore. Figure 8 shows the relative distances between the four property spheres that represent the essential functional groups for ligand binding. The distances are as follows: HA1–HA2, ~5.0 &ARING;; HA1–HP1, ~5.3 &ARING;; HA1–

HP2, ~5.5 &ARING;; HA2–HP1, 4.7 &ARING;; HA2–HP2, 3.2 &ARING;; and HP1–HP2, 4.8 &ARING;.

Estimation of the Ligand-Binding Site of Rat Mrp2

A good CoMFA model was identified with the following parameters: a q^2 value of 0.59 with six PLS components, an s_{press} value of 0.64, an r^2 value of 0.99, and a standard error of 0.08. We suggest that the success of the CoMFA was a result of the use of the molecular alignment obtained using SUPERPOSE. This represents a unique and distinctive approach, in which the binding conformation and 3D pharmacophore of a ligand are estimated using ligand-based drug design techniques and are then applied to the molecular alignment, which is essential to CoMFA.

On the basis of the 3D pharmacophore and the contour map obtained from the CoMFA calculation, we have estimated the structure of the ligand-binding site of rat Mrp2 (Fig. 9). The four primary binding sites correspond to the 3D pharmacophore, comprising the four functional groups that are essential for the binding of ligands to rat Mrp2. The model also suggests that secondary binding sites, which correspond to specific contour levels in the CoMFA contour map, are important in explaining the variation of the binding affinities of ligands to rat Mrp2.

In conclusion, we propose that both hydrophobic and electrostatic interactions have vital roles in the binding of ligands to rat Mrp2. Ligand recognition seems to be achieved through interactions in the two hydrophobic sites and the two electrostatically positive sites (primary binding sites). Moreover, the broad substrate specificity of rat Mrp2 might be achieved by combinations of the secondary binding sites (two electrostatically positive sites and two electrostatically negative sites) with the primary binding sites.

The method described here for determining the binding conformation of ligands represents a powerful tool in cases where ligands have the same binding mode to the target protein. Of course, it should be noted that different binding modes might exist for some ligands; however, all of the ligands used in this analysis appeared to have the same binding mode, according to the results of the CoMFA. We believe that our data will be useful in the development of new com-

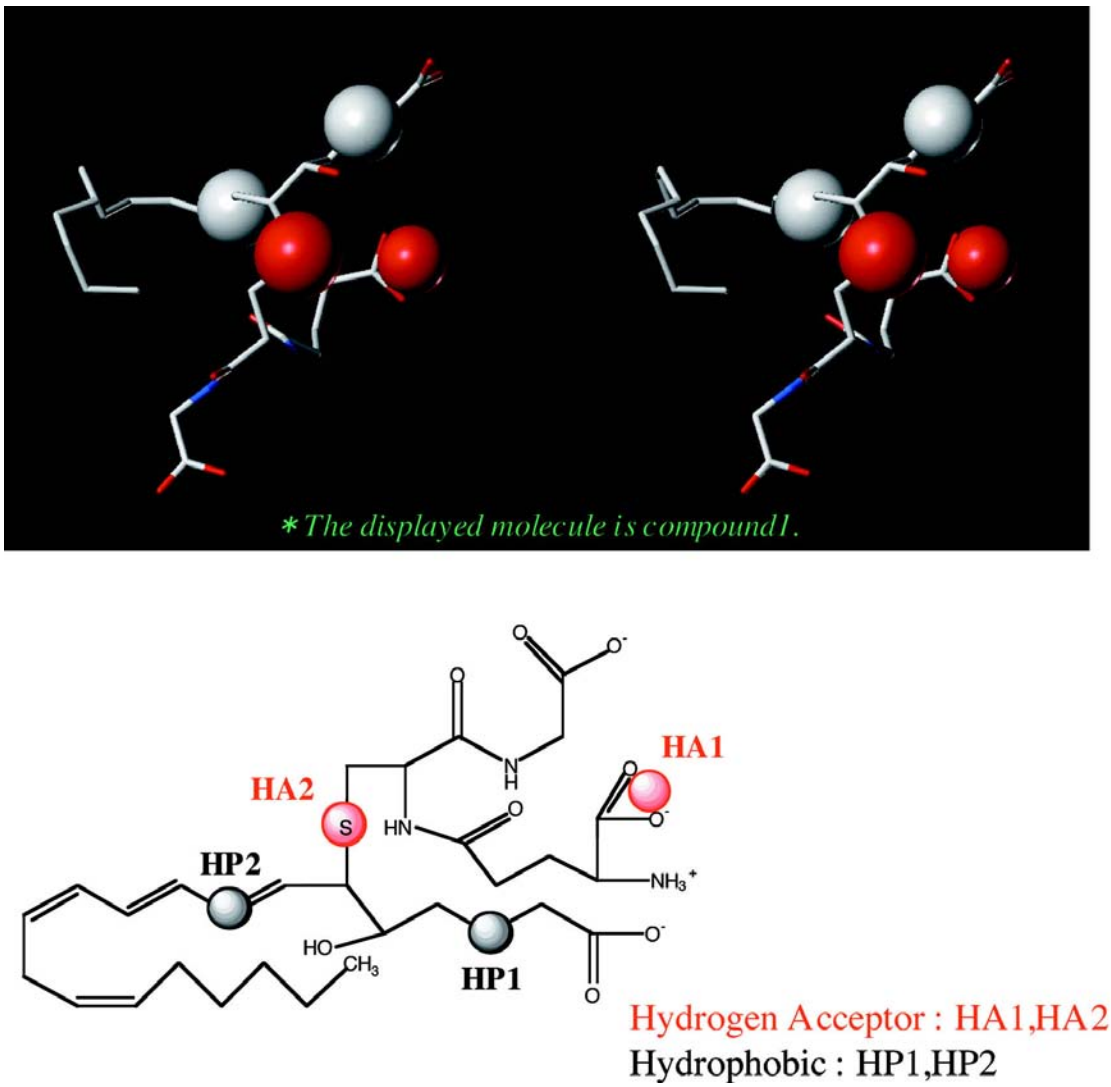

Fig. 7. A stereo view of the four property spheres that represent a 3D pharmacophore of ligands for Mrp2/ABCC2 and the 3D structure of compound **1** together with its structural formula.

pounds to control transport by Mrp2. We also predict that it will be possible to perform *in silico* screening for a range of compounds using the CoMFA QSAR model in order to evaluate their affinity for Mrp2.

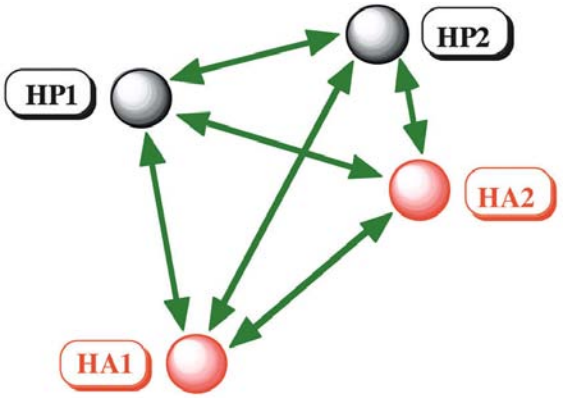

	Relative distances (Å)
HA1 - HA2	5.0 ± 0.9
HA1 - HP1	5.3 ± 0.7
HA1 - HP2	5.5 ± 1.6
HP1 - HA2	4.7 ± 0.8
HP1 - HP2	4.8 ± 1.1
HA2 - HP2	3.2 ± 1.2

Fig. 8. Relative distances between the four property spheres representing the functional groups that are essential for ligand binding.

REFERENCES

1. O. R. P. Elferink, D. K. Meijer, F. Kuipers, P. L. Jansen, A. K. Groen, and G. M. Groothuis. Hepatobiliary secretion of organic compounds; molecular mechanisms of membrane transport. *Biochim. Biophys. Acta* **1241**:215–268 (1995).
2. M. Yamazaki, H. Suzuki, and Y. Sugiyama. Recent advances in carrier-mediated hepatic uptake and biliary excretion of xenobiotics. *Pharm. Res.* **13**:497–513 (1996).
3. D. Keppler and J. Konig. Hepatic canalicular membrane 5: expression and localization of the conjugate export pump encoded by the *Mrp2* (*cMRP/cMOAT*) gene in liver. *FASEB J.* **11**:509–516 (1997).
4. K. Ito, H. Suzuki, T. Hirohashi, K. Kume, T. Shimizu, and Y. Sugiyama. Molecular cloning of canalicular multispecific organic anion transporter defective in EHBR. *Am. J. Physiol.* **272**:G16–G22 (1997).
5. C. C. Paulusma, P. J. Bosma, G. J. Zaman, C. T. Bakker, M. Otter, G. L. Scheffer, R. J. Scheper, P. Borst, and O. R. P. Elferink. Congenital jaundice in rats with a mutation in a multidrug resistance-associated protein gene. *Science* **271**:1126–1128 (1996).
6. K. Sathirakul, H. Suzuki, K. Yasuda, M. Hanano, O. Tagaya, T. Horie, and Y. Sugiyama. Kinetic analysis of hepatobiliary transport of organic anions in Eisai hyperbilirubinemic mutant rats. *J. Pharmacol. Exp. Ther.* **265**:1301–1312 (1993).
7. K. Sathirakul, H. Suzuki, T. Yamada, M. Hanano, and Y. Sugiyama. Multiple transport systems for organic anions across the bile canalicular membrane. *J. Pharmacol. Exp. Ther.* **268**:65–73 (1994).
8. M. Yamazaki, S. Akiyama, K. Ni'inuma, R. Nishigaki, and Y. Sugiyama. Biliary excretion of pravastatin in rats: contribution of the excretion pathway mediated by canalicular multispecific organic anion transporter. *Drug Metab. Dispos.* **25**:1123–1129 (1997).
9. H. Ishizuka, K. Konno, H. Naganuma, K. Sasahara, Y. Kawahara, K. Niinuma, H. Suzuki, and Y. Sugiyama. Temocaprilat, a novel angiotensin-converting enzyme inhibitor, is excreted in bile via an ATP-dependent active transporter (cMOAT) that is deficient in

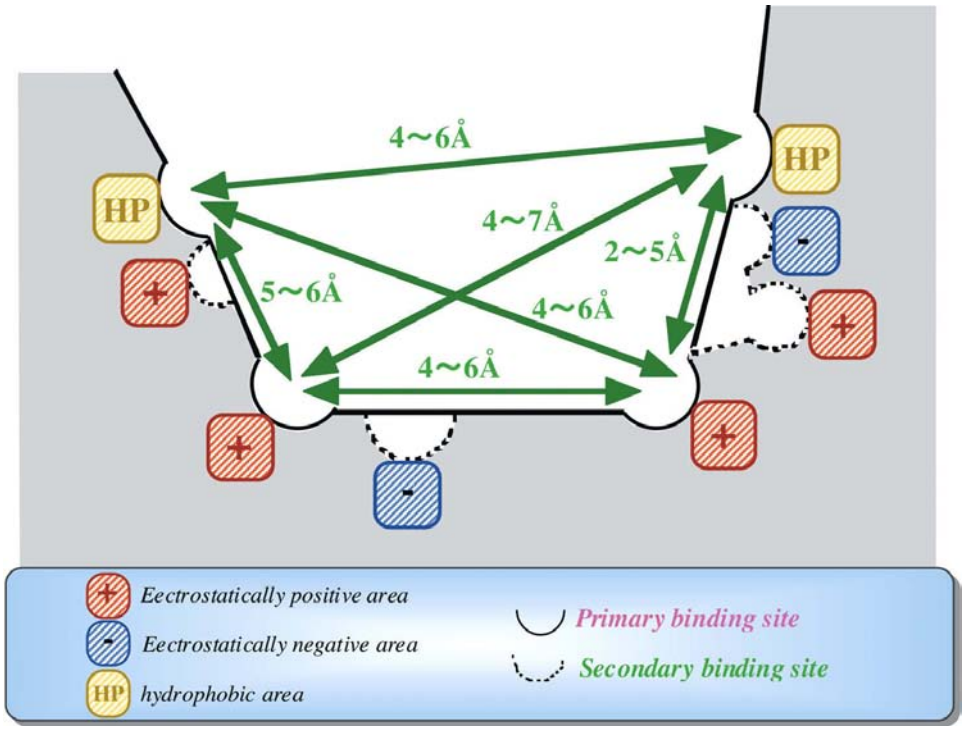

Fig. 9. Ligand-binding region of Mrp2/ABCC2 estimated using the 3D pharmacophore and CoMFA contour map.

Eisai hyperbilirubinemic mutant rats (EHBR). *J. Pharmacol. Exp. Ther.* **280**:1304–1311 (1997).
10. H. C. Shin, Y. Kato, T. Yamada, K. Niinuma, A. Hisaka, and Y. Sugiyama. Hepatobiliary transport mechanism for the cyclopentapeptide endothelin antagonist BQ-123. *Am. J. Physiol.* **272**: G979–G986 (1997).
11. T. Ishikawa, M. Muller, C. Klunemann, T. Schaub, and D. Keppler. ATP-dependent primary active transport of cysteinyl leukotrienes across liver canalicular membrane. Role of the ATP-dependent transport system for glutathione S-conjugates. *J. Biol. Chem.* **265**:19279–19286 (1990).
12. K. Kobayashi, Y. Sogame, H. Hara, and K. Hayashi. Mechanism of glutathione S-conjugate transport in canalicular and basolateral rat liver plasma membranes. *J. Biol. Chem.* **265**:7737–7741 (1990).
13. T. Nishida, Z. Gatmaitan, J. Roy-Chowdhry, and I. M. Arias. Two distinct mechanisms for bilirubin glucuronide transport by rat bile canalicular membrane vesicles. Demonstration of defective ATP-dependent transport in rats (TR-) with inherited conjugated hyperbilirubinemia. *J. Clin. Invest.* **90**:2130–2135 (1992).
14. O. Takenaka, T. Horie, K. Kobayashi, H. Suzuki, and Y. Sugiyama. Kinetic analysis of hepatobiliary transport for conjugated metabolites in the perfused liver of mutant rats (EHBR) with hereditary conjugated hyperbilirubinemia. *Pharm. Res.* **12**:1746–1755 (1995).
15. M. Trauner, M. Arrese, C. J. Soroka, M. Ananthanarayanan, T. A. Koeppel, S. F. Schlosser, F. J. Suchy, D. Keppler, and J. L. Boyer. The rat canalicular conjugate export pump (Mrp2) is down-regulated in intrahepatic and obstructive cholestasis. *Gastroenterology* **113**:255–264 (1997).
16. X. Y. Chu, Y. Kato, and Y. Sugiyama. Multiplicity of biliary excretion mechanisms for irinotecan, CPT-11, and its metabolites in rats. *Cancer Res.* **57**:1934–1938 (1997).
17. H. Suzuki and Y. Sugiyama. Role of transporters in the detoxification of xenobiotics: recent advances in the study of cMOAT/MRP. *Tanpakushitsu Kakusan Koso* **42**:1273–1284 (1997).
18. H. Tsujishita and S. Hirono. CAMDAS: an automated conformational analysis system using molecular dynamics. *J. Comput. Aided Mol. Des.* **11**:305–315 (1997).
19. K. Iwase and S. Hirono. Estimation of active conformations of drugs by a new molecular superposing procedure. *J. Comput. Aided Mol. Des.* **13**:499–512 (1999).
20. R. D. Cramer, D. E. Patterson, and J. D. Bunce. Comparative molecular field analysis (CoMFA). 1. Effect of shape on binding of steroids to carrier proteins. *J. Am. Chem. Soc.* **110**:5959–5967 (1988).
21. N. L. Allinger. Conformational analysis. 130. MM2. A hydrocarbon force field utilizing V1 and V2 torsional terms. *J. Am. Chem. Soc.* **99**:8127–8134 (1977).
22. H. Suzuki and Y. Sugiyama. Transporters for bile acids and organic anions. *Pharm. Biotechnol.* **12**:387–439 (1999).